JOURNAL OF CATALYSIS 28, 428–441 (1973)

The Decomposition of Nitrous Oxide on Neodymium Oxide, Dysprosium Oxide and Erbium Oxide

JOHN F. READ

Department of Chemistry, Mount Allison University,
Sackville, New Brunswick, Canada

Received July 27, 1972

The decomposition of nitrous oxide on neodymium oxide, dysprosium oxide and erbium oxide has been studied in two pressure ranges of approximately 1 to 10 Torr and 10 to 100 Torr, over a temperature range of 400 to 600°C. In all cases, the kinetics are first-order in nitrous oxide with a pseudo-rate constant varying with initial pressure. This effect is more noticeable at low pressures, with the pseudo-rate constant decreasing as the initial pressure of nitrous oxide is increased at a constant temperature.

The results have been explained by assuming that the rate-determining step is the surface decomposition of nitrous oxide. Oxygen desorption is also an important rate-controlling step, particularly at high oxygen pressures. There is a reversible deactivation of a fraction of the initially active sites by adsorbed oxygen formed from the nitrous oxide. This deactivation is dependent upon initial pressure.

INTRODUCTION

The decomposition of nitrous oxide is one of the simplest reactions in heterogeneous catalysis, and many studies have been made of the kinetics and mechanism over metal oxides. Nevertheless, there is no overall consistency in the results, particularly with respect to the kinetic and pretreatment effects of oxygen. The purpose of this contribution is to provide more data on the decomposition of nitrous oxide over selected lanthanide oxides as a basis for a comparison of the results across the series. The effect of the gradual change in properties of the lanthanide oxides on the kinetics of the reaction should provide valuable evidence concerning the overall mechanism.

Many of the published results for the decomposition of nitrous oxide have been explained using simple first-order kinetics. However, examination of the data shows that in many cases a detailed kinetic study was not attempted. For example, first-order kinetics were assumed over chromium(III)oxide–aluminum(III)oxide (*1*) and cobalt(II)oxide (*2*); the kinetics were studied in excess oxygen over cobalt(II)oxide, copper(II)oxide and nickel(II)oxide (*3*); only the initial stages of the reaction were studied over nickel(II)oxide (*4*); the initial pressure was not varied over iron(III)oxide (*5*). Detailed kinetic studies often reveal a retarding effect for oxygen, and the kinetic expression frequently involves a negative half-order dependence on oxygen pressure, for example (*6–8*). The mechanism usually involves the surface decomposition of nitrous oxide as the rate-determining step, with the desorption of oxygen as an important step.

Several studies have been made of the nitrous oxide decomposition on lanthanide oxides, although a detailed analysis of the kinetics has not been attempted. Cremer and Marschall (*9*) found that the kinetics were first-order during the initial stages of the reaction over lanthanum oxide, and Saito, Yoneda and Makishima (*10*) assumed first-order kinetics over neodymium oxide. Winter (*11*) used the kinetic expression

$$-\frac{dP_{N_2O}}{dt} = k\frac{P_{N_2O}}{(P_{O_2})^{1/2}}$$

to analyze the results for the decomposition over lanthanide oxides pretreated with oxygen.

This contribution extends the work of Winter to provide a detailed analysis of the effect of pressure, pretreatment and added gases on the overall kinetics of the decomposition of nitrous oxide on neodymium oxide, dysprosium oxide and erbium oxide.

EXPERIMENTAL METHODS

The apparatus comprised a conventional high-vacuum system. In the pressure range 1 to 10 Torr, the total pressure was measured using a McLeod gauge. To ensure that the reaction was not diffusion-controlled, a glass, propeller-driven, circulating pump was included for some of the runs, and various amounts of catalyst were used. In the pressure range 10 to 100 Torr, the total pressure was measured using a compression manometer. A glass piston pump, similar to that described by Watson (*12*), was included for all runs, providing a continual flow of gas over the catalyst.

The reaction was followed by measuring the increase in total pressure in the closed reaction chamber every 4 min. The piston pump was stopped when the pressure was being measured. A trap, surrounded by an acetone–dry ice mixture, protected the catalyst from contamination.

The nitrous oxide (supplied by The British Oxygen Co.) was purified by successive condensation and evaporation at liquid nitrogen temperatures, the impurities being separated from the solid nitrous oxide. Water was condensed from the gaseous nitrous oxide by using a trap surrounded by an acetone–dry ice mixture. Spectroscopically pure helium and oxygen were obtained from The British Oxygen Co.

The catalysts used in the present study were neodymium oxide, dysprosium oxide and erbium oxide of Specpure grade supplied by Johnson Matthey. X-Ray and ir analysis confirmed that all three oxides possessed the *C*-type structure (*13*) and that there was no change in structure during the experiments. The neodymium oxide appeared to be hydrated (*14*). Surface areas were measured by the BET method using krypton.

The oxides were conditioned by heating for 7 days at 550°C and $<10^{-6}$ Torr. For runs at temperatures above 550°C, the oxides were heated at the reaction temperature and $<10^{-6}$ Torr for at least 12 hr before commencing the reaction. Reproducible results were obtained by evacuating the system for 5 min between runs at the same temperature and at least 2 hr between runs at different temperatures. Runs were followed for about 1 hr or about 60% decomposition.

The reaction was studied over the temperature range 400 to 600°C and over the two pressure ranges of 1 to 10 Torr and 10 to 100 Torr. Various initial pressures of nitrous oxide were used, often with other gases added initially with the nitrous oxide.

RESULTS

The experimental data were analyzed using the general equation

$$-\frac{dP_A}{dt} = kP_A, \qquad (1)$$

where P_A is the pressure of nitrous oxide (Torr), t is the time (sec) and k is the pseudo-first-order rate constant. The initial pressure of nitrous oxide, $(P_A)_{t\to 0}$, was determined by experimental measurement and extrapolation. The rate constant used in this paper is the absolute pseudo-first-order rate constant at a particular initial pressure of nitrous oxide, k_{abs}, with

$$k_{\text{abs}} = \frac{kV}{60A}, \qquad (2)$$

where V is the effective volume of the system (m^3) and A is the total surface area of the catalyst (m^2).

Runs are labeled by indicating with the first letter the oxide, and with the second letter the pressure range. That is, runs over neodymium oxide in the lower pressure range (1 to 10 Torr) are represented by NL, and runs over dysprosium oxide in the higher pressure range (10 to 100 Torr) are represented by DH. A series refers to a set of runs performed together at a particular temperature.

For all runs, the first-order plots were linear up to at least 30% decomposition (see Table 1) with a pseudo-rate constant dependent on the initial pressure of nitrous oxide. In the pressure range 1 to 10 Torr, the linearity was usually maintained for more than 30% decomposition, and the pseudo-rate constant always decreased as the initial pressure of nitrous oxide was increased at a constant temperature. In the pressure range 10–100 Torr, the initial pressure effect on the pseudo-rate constant was less pronounced and, in some cases, it was masked by experimental error. Gases initially added with the nitrous oxide caused the pseudo-rate constant to decrease.

Ten runs were taken to completion and in all cases the experimentally measured increase in pressure was slightly less than, or equal to, the theoretically predicted increase.

The results in each pressure range over each catalyst are presented below and summarized in Table 1.

Pressure Range 1 to 10 Torr

Neodymium Oxide

Preliminary measurements were made using a sample which had been used in previous experiments. The activation energy from the Arrhenius plot, using a constant initial pressure of approximately 2 Torr, is 31 ± 2 kcal mole^{-1}.

The results from a detailed study on a fresh sample are summarized in Table 2. $(P_B)_{t\to 0}$ is the pressure of oxygen added initially with the nitrous oxide, and the number in parentheses after the run indicates the number of identical runs performed at that pressure and temperature. The typical results for Series NL10 at 439°C are shown in Fig. 1. The Arrhenius plot is shown in Fig. 2. The line is drawn through points corresponding to an initial pressure of approximately 1 Torr. Lines with similar slopes are obtained by joining other points corresponding to equal initial pressures of nitrous oxide. The activation energy is 14 ± 2 kcal mole^{-1}. First-order plots were still obtained when initially-added oxygen was present. At a constant initial pressure of nitrous oxide the slope of the plot decreases as the pressure of initially-added oxygen is increased. After series NL 11 had been completed,

TABLE 1
SUMMARY OF RESULTS

Catalyst	Total surface area (m^2)	Pressure range (Torr)	Temp range (°C)	Percentage reaction first-order (%)	Order with respect to concn	Activation energy (kcal mole^{-1})	Pretreatment
Nd_2O_3	2.9	0.2–4	440–508	60		31 ± 2	Impurities
	3.2	0.7–4	439–524	60	0.6	14 ± 2	None
	1.9	10–90	397–604	30	0.9	22 ± 1	None
	1.9	10–90	409–590	30		14 ± 1	Oxygen
	1.9	30–40	439–504	30		30 ± 3	Impurities
Dy_2O_3	0.8	0.6–6	450–550	50	0.7	27 ± 2	None
	0.6	20–80	541–604	30	0.9	23 ± 3	None
Er_2O_3	0.8	1–5	433–554	40	0.8	18 ± 3	None
	0.8	1–5	439–554	40		24 ± 2	Impurities
	1.0	10–80	479–615	50	1.0	28 ± 2	None
	1.0	10–30	514–610	50		19 ± 2	Oxygen

TABLE 2
NITROUS OXIDE DECOMPOSITION ON NEODYMIUM OXIDE[a]

Run	Temp (°C)	$(P_A)_{t\to 0}$ (Torr)	$(P_B)_{t\to 0}$ (Torr)	$k_{abs} \times 10^7$ (m sec^{-1})
NL 1 (2)	452	1.02		0.81
NL 2 (3)	485	1.01		1.42
NL 3 (2)	496	1.03		1.47
NL 4 (2)	509	1.01		1.77
NL 5 (2)	524	1.01		2.06
NL 6 (2)	516	1.00		1.84
NL 7.1 (3)	502	0.88		1.69
7.2 (1)		1.57		1.29
7.3 (1)		2.99		0.94
NL 8 (2)	476	0.78		1.31
NL 9.1 (3)	458	0.77		0.92
9.2 (1)		2.22		0.70
9.3 (1)		3.57		0.57
NL 10.1 (2)	439	0.75		0.66
10.2 (1)		2.14		0.54
10.3 (1)		3.48		0.42
NL 11.1 (1)	523	1.95	2.05	2.05
11.2 (1)		1.91	0.39	2.53
11.3 (1)		1.74	6.00	1.40
11.4 (1)		1.84	2.33	1.96

[a] Pressure range, 1-10 Torr; $A = 3.2$ m^2, $V = 6.57 \times 10^{-4}$ m^3.

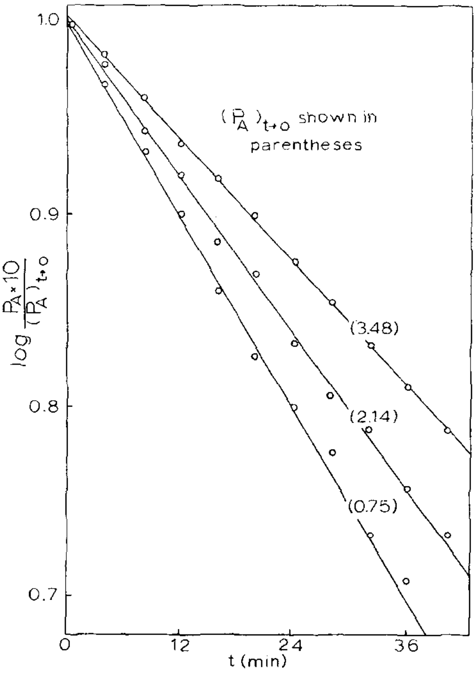

FIG. 1. First-order plots for the decomposition of nitrous oxide over neodymium oxide at 439°C (series NL10).

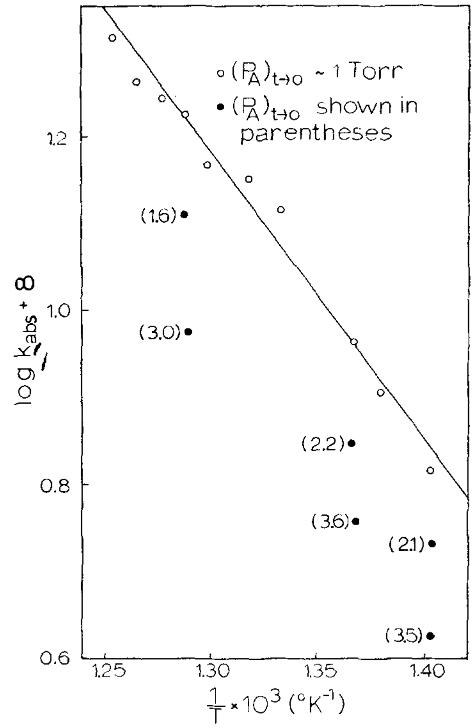

FIG. 2. Arrhenius plot for the decomposition of nitrous oxide over neodymium oxide in the pressure range 1 to 10 Torr.

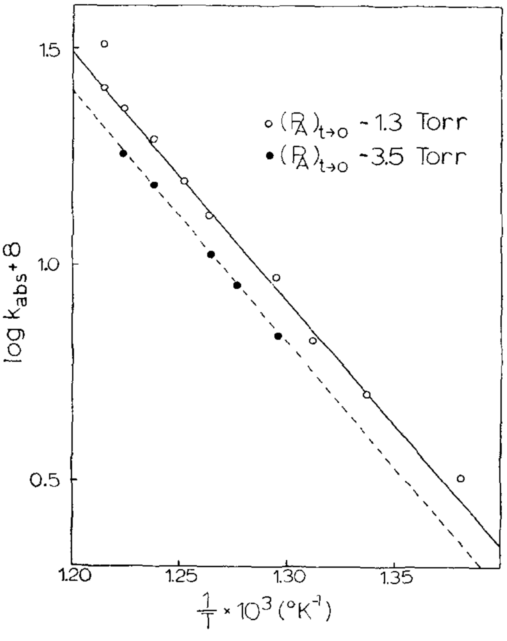

FIG. 3. Arrhenius plot for the decomposition of nitrous oxide over dysprosium oxide in the pressure range 1 to 10 Torr.

the carbon dioxide–acetone bath protecting the catalyst was removed. The sample became far less active, and the activity could be only partially regained after prolonged heating at 550°C and $<10^{-6}$ Torr.

TABLE 3
Nitrous Oxide Decomposition on Dysprosium Oxide[a]

Run	Temp (°C)	$(P_A)_{t\to 0}$ (Torr)	$k_{\text{abs}} \times 10^7$ (m sec^{-1})
DL 1 (3)	550	1.40	3.27
DL 2 (2)	420	1.41	Curved
DL 3.1 (2)	451	1.40	0.32
3.2 (1)		2.73	0.29
3.3 (1)		4.00	0.29
DL 4.1 (3)	475	1.37	0.50
4.2 (1)		2.66	0.47
4.3 (1)		3.91	0.46
DL 5.1 (3)	510	1.34	1.00
5.2 (1)		2.58	1.00
5.3 (1)		3.81	0.91
DL 6.1 (3)	527	1.30	1.56
6.2 (1)		2.53	1.56
6.3 (1)		3.73	1.33
DL 7.1 (2)	544	1.26	2.31
7.2 (1)		2.47	2.07
7.3 (1)		3.64	1.83
7.4 (1)		5.76 +2.26(N_2) +1.13(O_2)	1.50
DL 8.1 (3)	535	1.23	1.95
8.2 (1)		2.37	1.82
8.3 (1)		3.50	1.54
DL 9.1 (3)	518	1.20	1.29
9.2 (1)		2.31	1.22
9.3 (1)		3.42	1.06
9.4 (1)		5.49 +1.19(N_2) +0.60(O_2)	0.82
DL 10.1 (3)	499	0.62	0.77
10.2 (1)		1.14	0.95
10.3 (1)		2.24	0.77
10.4 (1)		3.69 +0.70(N_2) +0.35(O_2)	0.68
DL 11.1 (3)	489	1.12	0.67
11.2 (1)		1.96 +0.24(N_2) +0.12(O_2)	0.66
DL 12 (2)	550	1.10	2.60

[a] Pressure range, 1–10 Torr; $A = 0.8$ m^2, $V = 6.62 \times 10^{-4}$ m^3.

Dysprosium Oxide

The results are summarized in Table 3. Four runs (DL 7.4, DL 9.4, DL 10.4 and DL 11.2) were performed by adding an extra amount of nitrous oxide before the previous run was completed. The Arrhenius plot is shown in Fig. 3 giving an activation energy of 27 ± 2 kcal mole^{-1} at a constant initial pressure of nitrous oxide.

Erbium Oxide

The results are summarized in Table 4. Below 460°C, the total pressure in the system remained constant for a few minutes at the start of the reaction, and then first-order kinetics were obeyed. After completion of series EL 7, the carbon dioxide–acetone bath was temporarily removed. The effect of this can be seen in the Arrhenius plots of Fig. 4. At a constant initial pressure of approximately 1.5 Torr, the activation

TABLE 4
Nitrous Oxide Decomposition on Erbium Oxide[a]

Run	Temp (°C)	$(P_A)_{t\to 0}$ (Torr)	$k_{\text{abs}} \times 10^7$ (m sec^{-1})
EL 1 (3)	554	1.70	4.29
EL 2.1 (3)	433	1.68	0.66
2.2 (1)		4.89	0.48
2.3 (1)		3.29	0.47
EL 3.1 (3)	450	1.64	0.76
3.2 (1)		3.24	0.60
3.3 (1)		4.72	0.55
EL 4.1 (3)	475	1.60	1.14
4.2 (1)		3.13	0.96
4.3 (1)		4.61	0.81
EL 5 (3)	504	1.56	1.78
EL 6.1 (3)	534	1.55	2.80
6.2 (1)		3.03	2.36
6.3 (1)		4.45	1.99
EL 7.1 (3)	516	1.51	2.07
7.2 (1)		2.95	1.73
7.3 (1)		4.34	1.56
EL 8 (3)	486	1.46	1.02
EL 9.1 (3)	460	1.45	0.59
9.2 (1)		2.84	0.54
9.3 (1)		4.18	0.52
EL 10 (3)	439	1.42	0.35
EL 11 (1)	554	1.40	4.15

[a] Pressure range, 1–10 Torr; $A = 0.8$ m^2, $V = 6.52 \times 10^{-4}$ m^3.

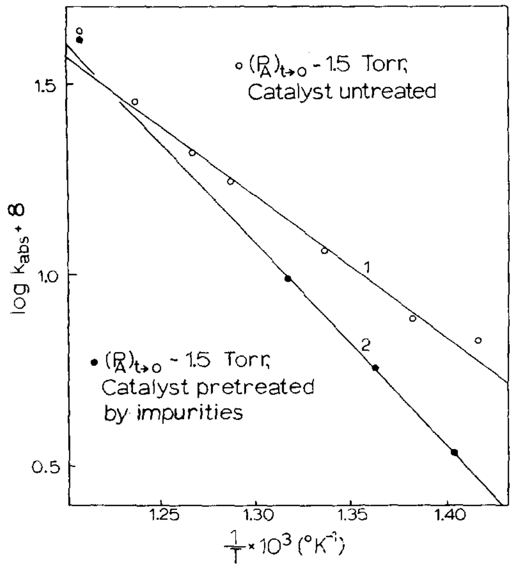

FIG. 4. Arrhenius plots for the decomposition of nitrous oxide over erbium oxide in the pressure range 1 to 10 Torr.

energy changes from 18 ± 3 (line 1) to 24 ± 2 kcal mole^{-1} (line 2) as a result of pretreatment by impurities. The pseudo-rate constants from runs EL 1 and EL 2.1 are relatively higher than the pseudo-rate constants from subsequent runs.

Pressure Range 10 to 100 Torr

Neodymium Oxide

The results are summarized in Table 5. For runs NH 18.4, NH 19.5 and NH 20.5, a discharge was passed for 30 min through oxygen over the catalyst before the nitrous oxide was added. This process is indicated in Table 5 by (O). At 397 and 421°C the total pressure in the system remained constant for a few minutes at the start of the reaction, and then first-order kinetics were obeyed. In series NH 1, the pseudo-rate constant decreased with successive runs. After completion of series NH 20, the carbon dioxide–acetone bath was removed, the catalyst being at room temperature. Runs NH 21 to 26 were performed after the catalyst had been left in air for 3 wk and then heated at 480°C for 12 hr at $<10^{-6}$ Torr.

TABLE 5
NITROUS OXIDE DECOMPOSITION ON NEODYMIUM OXIDE[a]

Run	Temp (°C)	$(P_A)_{t\to 0}$ (Torr)	Initial pressure of gases other than nitrous oxide (Torr)	$k_{abs}\times 10^8$ (m sec^{-1})
NH 1.1	397	27.3		0.72
1.2		61.6		0.68
1.3		28.1		0.46
1.4		51.7		0.38
NH 2.1	421	26.9		1.08
2.2		51.4		1.05
2.3		69.4		0.82
2.4		93.6		0.80
NH 3.1	440	26.7		1.66
3.2		37.0		1.53
3.3		62.6		1.46
3.4		88.8		1.35
NH 4.1	456	26.0		2.65
4.2		35.9		2.53
NH 5.1	479	25.4		3.57
5.2		35.5		3.38
5.3		79.0		3.02
NH 6.1	499	25.6		5.28
6.2		56.2		5.18
6.3		68.2		4.71
NH 7.1	517	24.7		7.69
7.2		46.4		7.20
7.3		80.3		5.36
NH 8.1	536	25.1		10.00
8.2		34.6		10.10
NH 9.1	552	15.8		12.97
9.2		51.9		10.73
9.3		81.7		10.76
9.4		36.6		11.61
9.5		16.7		14.28
NH 10.1	576	13.1		19.90
10.2		29.0		16.59
10.3		35.6		13.80
10.4		41.4		13.08
10.5		58.3		12.99
10.6		73.7		11.41
10.7		86.9		11.08
NH 11.1	593	23.5		26.37
11.2		33.4		15.70
NH 12.1	604	15.1		28.05
12.2		29.3		24.03
12.3		39.6	25.4 (N_2) 12.7 (O_2)	14.32
12.4		41.0		19.71
NH 13.1	566	30.4		18.62
13.2		30.2	3.6 (O_2)	13.14

TABLE 5 (*Continued*)

Run	Temp (°C)	$(P_A)_{t\to 0}$ (Torr)	Initial pressure of gases other than nitrous oxide (Torr)	$k_{abs} \times 10^8$ (m sec^{-1})
13.3		29.7	12.9 (O_2)	12.49
13.4		29.4	16.7 (O_2)	12.43
NH 14.1	518	31.4		8.60
14.2		31.4	2.4 (O_2)	8.48
14.3		30.8	7.9 (O_2)	8.13
14.4		30.2	13.0 (O_2)	8.09
NH 15.1	492	29.6	1.9 (O_2)	6.16
15.2		29.1	6.0 (O_2)	6.28
15.3		28.6	11.1 (O_2)	5.70
15.4		28.0		6.32
NH 16.1	450	27.3	3.3 (O_2)	3.31
16.2		27.5	6.1 (O_2)	3.10
16.3		26.8	9.4 (O_2)	3.01
16.4		26.2		3.83
16.5		37.0	5.3 (O_2) 10.5 (N_2)	2.67
NH 17.1	409	90.5		1.28
17.2		56.9		1.24
17.3		35.8		1.43
NH 18.1	504	23.9		7.67
18.2		15.9	7.4 (O_2) 14.8 (N_2)	6.61
18.3		23.7	4.3 (O_2)	6.92
18.4		23.1	4.3 (O)	5.02
NH 19.1	535	22.6		10.89
19.2		13.4	8.4 (O_2) 16.8 (N_2)	7.16
19.3		22.5	5.7 (O_2)	9.19
19.4		21.9	5.9 (air)	9.92
19.5		20.8	5.2 (O)	10.87
NH 20.1	590	21.0		24.00
20.2		13.1	8.8 (O_2) 17.5 (N_2)	8.95
20.3		20.3	5.0 (O_2)	24.00
20.4		19.9	7.0 (air)	20.15
20.5		19.5	4.3 (O)	24.00
NH 21	439	37.5		1.11
NH 22	453	37.5		2.24
NH 23	470	37.3		2.88
NH 24	475	36.3		3.35
NH 25	489	36.2		4.15
NH 26	504	35.8		5.24

[a] Pressure range, 10–100 Torr; $A = 1.9$ m^2, $V = 4.80 \times 10^{-4}$ m^3.

The Arrhenius plots are shown in Fig. 5. Line 1 joins points corresponding to an initial pressure of nitrous oxide of approximately 30 Torr from runs NH 1.1 to 13.1 inclusive (before the catalyst had been exposed to initially-added oxygen). An activation energy of 22 ± 1 kcal mole^{-1} is obtained. Line 2 joins points corresponding to the same constant initial pressure of nitrous oxide when only nitrous oxide was initially present but after the catalyst had been exposed to initially-added oxygen. Runs 14.1 to 20.1 inclusive give an activation energy of 14 ± 1 kcal mole^{-1}. Line 3 joins points corresponding to an initial

TABLE 6

NITROUS OXIDE DECOMPOSITION ON DYSPROSIUM OXIDE[a]

Run	Temp (°C)	$(P_A)_{t\to 0}$ (Torr)	$k_{abs} \times 10^8$ (m sec^{-1})
DH 1.1	604	42.5	6.60
1.2		46.8	7.25
1.3		62.6	7.20
1.4		24.2	7.57
DH 2.1	592	24.2	6.72
2.2		41.1	6.36
2.3		44.9	6.39
2.4		60.1	6.24
DH 3.1	587	23.9	7.08
3.2		45.1	5.74
3.3		60.4	5.18
3.4		80.5	6.24
DH 4.1	579	23.3	6.06
4.2		43.5	5.74
4.3		58.1	5.60
4.4		77.9	4.95
DH 5.1	569	22.7	5.80
5.2		42.5	5.64
5.3		57.2	5.15
5.4		76.9	4.49
DH 6.1	562	22.0	4.78
6.2		41.0	4.71
6.3		55.1	4.41
6.4		74.1	4.10
DH 7.1	574	21.4	5.68
7.2		39.5	5.53
7.3		53.1	5.80
7.4		72.0	5.03
DH 8.1	599	20.7	9.31
8.2		38.8	8.78
8.3		52.4	7.80
8.4		69.6	7.59
DH 9.1	549	38.3	4.14
9.2		51.4	3.52
9.3		69.1	3.85

[a] Pressure range, 10–100 Torr; $A = 0.6$ m^2, $V = 4.85 \times 10^{-4}$ m^3.

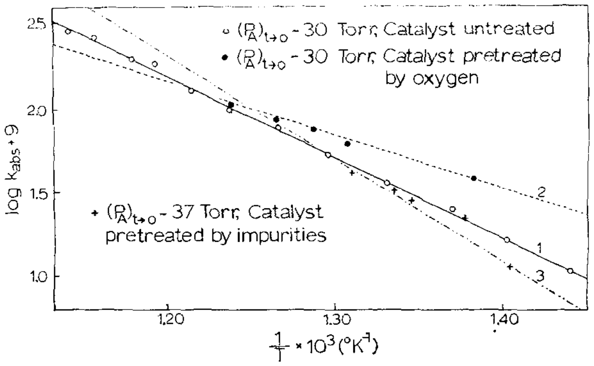

FIG. 5. Arrhenius plots for the decomposition of nitrous oxide over neodymium oxide in the pressure range 10 to 100 Torr.

pressure of nitrous oxide of approximately 37 Torr from runs NH 21 to 26 inclusive (after the catalyst had been exposed to impurities). The activation energy is 30 ± 3 kcal mole^{-1}.

Dysprosium Oxide

The results are summarized in Table 6. The Arrhenius plot, shown in Fig. 6, gives an activation energy of 23 ± 3 kcal mole^{-1} by joining points corresponding to a particular initial pressure of nitrous oxide.

Erbium Oxide

The results are summarized in Table 7. In series EH 1 to EH 9 inclusive (temp range, 479 to 550°C), the total pressure in the system usually remained constant for a few minutes at the start of the reaction and then first-order kinetics were obeyed. In addition, the pseudo-rate constant did not always show a pressure dependence. After run EH 20.4, the catalyst was heated at 550°C for 40 hr in 50 Torr of oxygen. The system was then evacuated for 4 min and series EH 21 was performed.

The Arrhenius plots are shown in Fig. 7. Line 1 joins points from series EH 1 to 15 inclusive (before the catalyst had been exposed to initially-added oxygen). Each point is the average value from all runs in that series. The activation energy is 28 ± 2 kcal mole^{-1}. Line 2 joins points corresponding to an initial pressure of nitrous oxide of approximately 20 Torr, when only nitrous oxide was initially present but after the catalyst had been exposed to initially-added oxygen. The activation energy is 19 ± 2 kcal mole^{-1}.

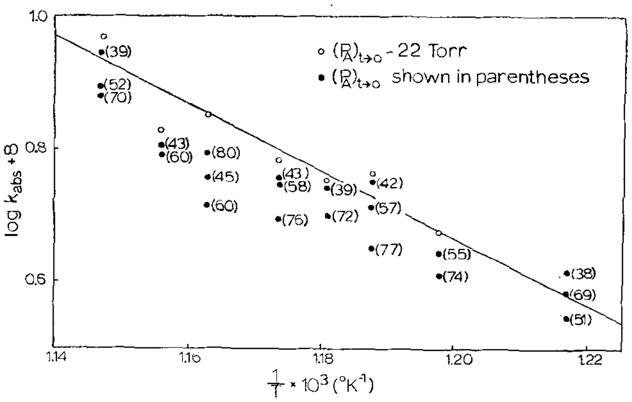

FIG. 6. Arrhenius plot for the decomposition of nitrous oxide over dysprosium oxide in the pressure range 10 to 100 Torr.

TABLE 7

NITROUS OXIDE DECOMPOSITION ON ERBIUM OXIDE[a]

Run	Temp (°C)	$(P_A)_{t\to 0}$ (Torr)	Initial pressure of gases other than nitrous oxide (Torr)	$k_{\mathrm{abs}} \times 10^8$ (m sec^{-1})
EH 1.1	514	35.5		2.34
1.2		47.8		2.48
1.3		65.0		2.25
EH 2.1	503	18.4		2.09
2.2		34.5		2.19
2.3		46.3		2.17
2.4		62.5		1.99
EH 3.1	492	34.2		1.85
3.2		46.0		1.75
3.3		62.0		1.55
3.4		76.7		1.48
EH 4.1	479	32.5		1.01
4.2		44.0		1.09
4.3		59.3		0.89
4.4		72.8		0.84
EH 5.1	509	31.8		2.68
5.2		42.6		2.30
5.3		57.3		2.37
EH 6.1	522	30.4		3.42
6.2		41.0		3.23
6.3		54.9		3.13
6.4		58.8		3.19
EH 7.1	533	16.2		4.40
7.2		30.4		4.19
7.3		40.7		4.24
7.4		54.8		4.23
EH 8.1	539	15.0		5.53
8.2		28.4		4.63
8.3		38.0		4.73
8.4		51.2		4.57
EH 9.1	550	28.5		5.89
9.2		38.3		6.31
9.3		51.7		5.69
9.4		27.4		6.23
EH 10.1	561	27.0		8.08
10.2		36.4		7.52
10.3		49.2		7.12
EH 11.1	571	14.2		11.13
11.2		26.6		10.00
11.3		35.9		9.80
11.4		48.3		9.50
EH 12.1	577	26.2		9.78
12.2		34.7		10.37
12.3		54.7		10.19
EH 13.1	587	25.2		13.32
13.2		34.3		11.98
13.3		54.1		11.60
13.4		24.3		13.61
EH 14.1	600	24.6		15.80
14.2		33.0		14.91
14.3		52.3		13.47
14.4		62.5		13.26
EH 15.1	615	12.9		20.29
15.2		28.3		18.57
15.3		42.8		17.68
15.4		54.4		15.52
EH 16.1	610	24.6	15.4 (O_2)	16.16
16.2		24.6	30.4 (O_2)	9.41
16.3		24.1	54.6 (O_2)	8.71
16.4		23.8		17.95
EH 17.1	595	23.0		14.66
17.2		23.3	13.4 (O_2)	12.67
17.3		22.8	25.9 (O_2)	10.41
17.4		22.8	47.8 (O_2)	7.41
EH 18.1	572	22.1		11.41
18.2		22.3	11.5 (O_2)	9.35
18.3		22.1	22.0 (O_2)	8.15
18.4		21.9	40.4 (O_2)	6.41
EH 19.1	544	20.9	9.7 (O_2)	7.14
19.2		21.2	27.3 (O_2)	5.24
19.3		20.8	41.0 (O_2)	4.76
19.4		20.7		7.44
EH 20.1	514	19.8		4.94
20.2		20.2	7.8 (O_2)	3.94
20.3		19.7	22.3 (O_2)	4.13
20.4		19.8	33.4 (O_2)	3.49
EH 21.1	550	18.1		6.90
21.2		31.1		6.90
21.3		40.3		6.40
21.4		46.3		6.20
EH 22.1	545	71.8	14.7 (N_2) 7.4 (O_2)	1.76
22.2		20.2	18.0 (O_2)	5.13
22.3		31.6	8.5 (O)	1.94

---

[a] Pressure range, 10–100 Torr; $A = 1.0$ m^2, $V = 4.82 \times 10^{-4}$ m^3.

DISCUSSION

Kinetics

A detailed analysis of the kinetic data by the cubic spline interpolation method

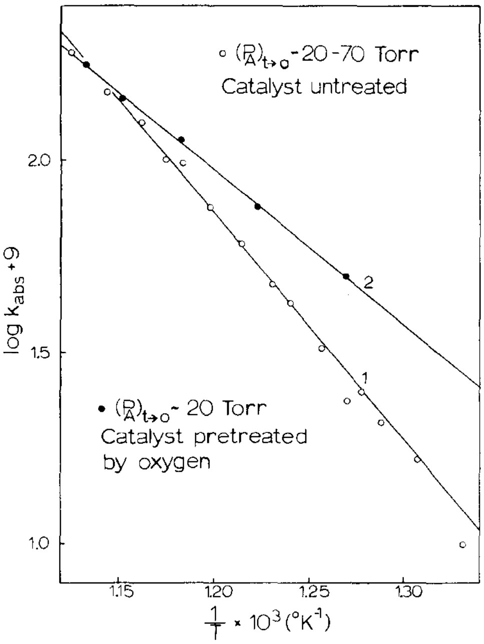

FIG. 7. Arrhenius plots for the decomposition of nitrous oxide over erbium oxide in the pressure range 10 to 100 Torr.

(*15*) showed that the best fit was obtained using a simple first-order kinetic expression with a pressure-dependent pseudo-first-order rate constant. The pressure dependence is of the form

$$\log k_{\text{abs}} = k_1 - k_2 \log(P_A)_{t\to 0}, \qquad (3)$$

where k_1 and k_2 are temperature-dependent constants. The results for neodymium oxide are shown in Fig. 8. Equation (3) is obeyed well within any particular pressure range, but linearity is not always maintained across the pressure ranges. This could be the result of a limiting factor in the pressure dependence.

Similar relationships to that shown in Eq. (3) have been observed by other workers for the nitrous oxide decomposition.

Linde, Margolis and Roginskii (*16*) found that, over cobalt–manganese spinels, the pseudo-first-order rate constant varied with initial pressure (0.08 to 0.64 Torr), according to the expression

$$k_{\text{abs}} = \frac{a}{(P_A)_{t\to 0}} + b, \qquad (4)$$

where $a = 0.003$ and $b = 0.001$.

Gay and Tompkins (*17*) found that an expression of the form shown in Eq. (3) was obeyed over nickel oxide in the pressure range 0.05 to 1 Torr between 22 and 140°C. The constants are temperature-independent, with $k_1 = 4$ and $k_2 = 0.6$.

Teichner has observed similar relationships for the oxidation of carbon monoxide. For example, Samaane and Teichner (*18*) observed the following relationship over nickel oxide–aluminum oxide:

$$k_{\text{abs}} = \frac{k_3}{(P)_{t\to 0}{}^{0.95}}, \qquad (5)$$

where k_3 is a temperature-dependent constant.

Winter (*11*) used a kinetic expression involving retardation by oxygen gas, that is,

$$k_{\text{abs}} = \frac{k_4}{(P_{O_2})^{1/2}}, \qquad (6)$$

where k_4 is a temperature-dependent constant. However, he did not attempt a detailed kinetic analysis, and he observed curves in some of his plots using Eq. (6). In addition, Winter calculated the rate constants at low pressures (2 Torr) directly from the rate constants obtained at high pressures (100 to 200 Torr). The present work shows that, as the pressure is increased, the pseudo-rate constant is less affected by initial pressure. Therefore, the pressure effect in the pressure range 100 to 200 Torr should be minimal.

The order with respect to concentration was determined from the initial-rate data, and it is shown for each oxide in Table 1. There is a slight tendency for the order to decrease as the temperature is increased in any particular pressure range, and, in all cases, the order is higher (and close to unity) in the higher pressure range. The fact that the order with respect to concentration differs from the order with respect to time further proves that the kinetics are not simple, particularly in the lower pressure range.

Activation Energies

The values for the activation energies are shown in Table 1. For the untreated

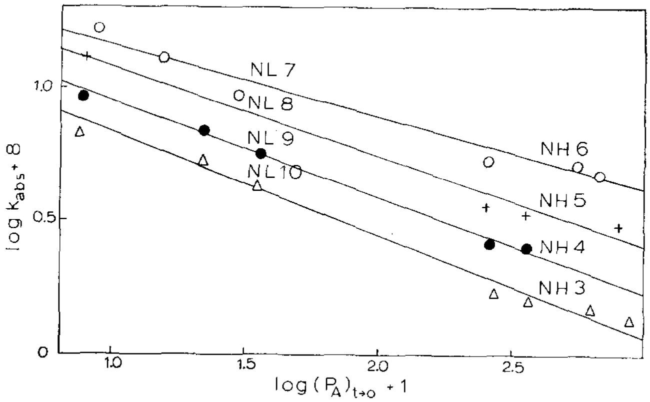

FIG. 8. Plot of Eq. (3) using the data from the decomposition of nitrous oxide over neodymium oxide.

catalysts, the activation energy remains constant within each pressure range. There is an increase in activation energy across the pressure ranges for neodymium oxide and erbium oxide, whereas the activation energy remains effectively constant for dysprosium oxide. The variation in activation energy with large pressure changes follows from Eley's Eq. (*19*)

$$E_a = E_t + \Delta H(1 - \theta), \qquad (7)$$

where E_a is the apparent activation energy, E_t is the true activation energy, ΔH is the heat of adsorption and θ is the fraction of the active surface that is covered. Large increases in pressure will increase θ and, therefore, increase the activation energy for exothermic processes. In the higher pressure range, the activation energy increases with decreasing ionic radius of the metal ion, but this trend is not observed in the lower pressure range. Hydrogen adsorption studies (*14*) have shown that the heat of adsorption and the equilibrium coverage increase with decreasing ionic radius. Therefore, according to Eq. (7), no systematic variation of activity is expected. Balandin and Tolstopiatova (*20*) have shown that the most regular pattern is obtained using bond energies. In Table 8, the values for the activation energies are compared to those obtained by Winter (*11*). The values compare favorably, showing the increase in activation energy with increasing pressure. The only discrepancy is in the low pressure value for neodymium oxide, where both the activation energy and the temperature range studied are lower than Winter's values. Bakumenko and Chashechnikova (*21*) found an anomalously high activity for neodymium oxide towards the oxidation of hydrogen and have explained this effect by the tendency for neodymium (III) oxide to form neodymium (V) oxide. This fact, together with the observation that pretreatment has a marked effect on

TABLE 8

COMPARISON OF ACTIVATION ENERGIES AND TEMPERATURE RANGES

	Activation energy (kcal mole^{-1})				Temp range studied (°C)	
Catalyst	1 to 6 Torr[a]	2 Torr[b]	10–90 Torr[a]	100–200 Torr[b]	[a]	[b]
Nd_2O_3	14	24	22	28	400–600	350–450
Dy_2O_3	27	27	23	36	450–600	450–600
Er_2O_3	18	21	28	40	450–600	530–630

[a] Results obtained in present work.

[b] Results obtained by Winter (*11*).

the bonding energy of oxygen with lanthanide oxides, for example (*22*), may explain the difference in the results.

In the higher pressure range over neodymium oxide and erbium oxide, the activation energy is irreversibly decreased to a value close to that observed in the lower pressure range, after the catalysts had been exposed to initially-added oxygen. Conversely, the activation energy is irreversibly increased after pretreatment by impurities (grease and mercury vapors). Over neodymium oxide, the value in both pressure ranges is increased to approximately 30 kcal mole^{-1}. This value is similar to the value of 32 kcal mole^{-1} obtained by Saito, Yoneda, and Makishima (*10*) in a flow system.

Effect of Initially-Added Gases

The effect of initially added gases was studied over neodymium oxide (both pressure ranges), dysprosium oxide (1 to 10 Torr pressure range), and erbium oxide (10 to 100 Torr pressure range).

When pure oxygen was initially-added, pseudo-first-order kinetics were still obeyed, with the pseudo-first-order rate constant decreasing as the initial pressure of oxygen was increased at a constant initial pressure of nitrous oxide. The relationship between the pseudo-rate constant and the pressure of oxygen was of the same form as shown in Eq. (3) although a slightly better fit was obtained using the expression without logarithms, namely

$$k_{\mathrm{abs}} = k_5 - k_6(P_{\mathrm{B}})_{t\to 0}, \qquad (8)$$

where k_5 and k_6 are constants.

Gases other than oxygen also decreased the pseudo-first-order rate constant, the effect being oxygen > air > additional dose of nitrous oxide = no gas initially added. The effect of oxygen through which a discharge had been passed was inconsistent, although the retarding effect was much greater than pure oxygen over erbium oxide in the 10 to 100 Torr pressure range.

Mechanism

The surfaces of the lanthanide oxides contain a large number of anion vacancies (approx 2.5×10^{18} m^{-2}) and it is probable that these centers, either separately or in clusters, form the active site for adsorption and catalysis.

Since it is known that both oxygen and nitrous oxide readily adsorb on the lanthanide oxides (*14*, *23*), a probable mechanism, involving adsorption onto F-centers, is:

$$\mathrm{N_2O(g)} + (\mathrm{e^-} \mid \square_s^-) \rightleftarrows (\mathrm{N_2O^-} \mid \square_s^-), \qquad (9)$$

$$(\mathrm{N_2O^-} \mid \square_s^-) \rightarrow \mathrm{N_2(g)} + (\mathrm{O^-} \mid \square_s^-), \qquad (10)$$

$$2(\mathrm{O^-} \mid \square_s^-) \rightleftarrows (\mathrm{e^-} \mid \square_s^-)(\mathrm{e^-} \mid \square_s^-) + \mathrm{O_2(g)}, \qquad (11)$$

$$\text{or} \quad 2(\mathrm{O^-} \mid \square_s^-) \rightleftarrows 2(\mathrm{e^-} \mid \square_s^-) + \mathrm{O_2(g)}. \qquad (12)$$

If the final step is (11), then F-centers will have to be regenerated from the R_2-centers. Assuming that the equilibria are readily established, the above mechanism would result in simple first-order kinetics.

The initial, irreversible, deactivation of a fraction of the active surface, observed for the first few runs over each oxide, is caused by the irreversible adsorption of oxygen ions formed from the nitrous oxide. The surfaces of the lanthanide oxides contain hydroxyl groups (*14*) and the irreversible adsorption could be the result of an extension of the crystal lattice:

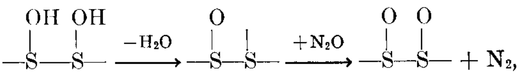

$$\overset{\mathrm{OH}}{\underset{|}{}}\!\!\!\!\!\!-\mathrm{S}-\overset{\mathrm{OH}}{\mathrm{S}}- \xrightarrow{-\mathrm{H_2O}} -\overset{\mathrm{O}}{\mathrm{S}}-\mathrm{S}- \xrightarrow{+\mathrm{N_2O}} -\overset{\mathrm{O}}{\mathrm{S}}-\overset{\mathrm{O}}{\mathrm{S}}- + \mathrm{N_2},$$

where S represents a surface site. The strong deactivating effect of grease and mercury vapors is the result of the blocking of F-centers (*22*).

The retarding effect of an increase in initial pressure of nitrous oxide is caused by the fast, reversible, deactivation of a fraction of the initially-active sites. The fact that a small amount of oxygen from the nitrous oxide is irreversibly adsorbed during the course of a reaction can be seen from the result that the total increase in pressure on completion of a reaction was equal to or less than that theoretically predicted, and from the appearance of a plateau in the total pressure versus time plots at low temperatures over two of the oxides. The reproducibility of consecutive runs indicates that the deactivation is reversible when the system is evacuated. It would appear that there is a limit to the fraction of surface that can be deactivated in this manner, resulting in the smaller effect of initial pressure on the pseudo-rate constant in the higher pressure range (10 to 100 Torr). The deactivation could be caused by adsorption onto isolated F-centers. If surface migration is slow, desorption will not occur according to Eqs. (11) or (12). Evacuation of the system will cause migration or incorporation, resulting in reactivation of the surface. Alternatively, deactivation may result from the formation of a more stable surface species from the $(\mathrm{O}^- \mid \square_s^-)$, for example:

$$(\mathrm{O}^- \mid \square_s^-) + (e^- \mid \square_s^-) \rightleftarrows (\mathrm{O}^{2-} \mid \square_s^-) + \square_s^-. \tag{13}$$

When the system is evacuated, the O^{2-} can desorb after migration, can be incorporated into the bulk of the catalyst, or can remain on the surface and convert an R_2-center into 2 F-centers:

$$(e^- \mid \square_s^-)(e^- \mid \square_s^-) + (\mathrm{O}^{2-} \mid \square_s^-) \rightleftarrows 2(e^- \mid \square_s^-) + (\mathrm{O}^{2-} \mid \square_s^-). \tag{14}$$

Gay (*24*) has shown that, after adsorption of nitrous oxide on nickel oxide, a peak appears in the desorption spectra which does not appear after oxygen adsorption. In addition, he found that the amount of oxygen desorbed was proportional to the logarithm of the pressure of nitrous oxide, and that it was probably an equilibrium process. In view of the similarity between the results in this paper and those of Gay and Tompkins (*17*), it is probable that the deactivation is the result of a process similar to that outlined in Eq. (13), and that reactivation results from the desorption of oxygen.

The retarding effect of initially-added oxygen could be due to the reverse of Eq. (11) or (12). It is known that oxygen is more strongly adsorbed than nitrous oxide (*14*, *23*) and that oxygen desorption is an important rate-controlling step (*11*). It is possible that this effect is not noticed for the low pressures of oxygen produced by the decomposition of nitrous oxide. Alternatively, the retarding effect could be caused by the irreversible adsorption of oxygen during the course of a reaction on a single or double F-center. The linearity of the pseudo-first-order plots with initially-added oxygen, and the drastic deactivation observed with oxygen through which a discharge had been passed over erbium oxide, support the suggestion that initially-added oxygen deactivates a fraction of the surface. The fact that the oxides used by Winter were pretreated with oxygen may account for the difference noted in the effect of pure oxygen during the course of a reaction.

The increase in activity seen over neodymium oxide and erbium oxide after exposure to initially-added oxygen is probably due to the ability of oxygen to create F-centers (active towards nitrous oxide decomposition) from R_2-centers (inactive towards nitrous oxide decomposition) by the reverse of Eq. (11) followed by (12). This probably occurs to a limited extent during a reaction but creation of F-centers is minimized by the presence of oxygen. It is unlikely that exposure to oxygen will cause nitrous oxide decomposition by the following mechanism:

$$\mathrm{N_2O(g)} + (\mathrm{O}^- \mid \square_s^-) \rightarrow \mathrm{N_2(g)} + \mathrm{O_2(g)} + (e^- \mid \square_s^-) \tag{15}$$

because this would minimize the retarding effect of initially-added oxygen during the course of a reaction.

CONCLUSION

The decomposition of nitrous oxide over neodymium oxide, dysprosium oxide and erbium oxide obeys pseudo-first-order kinetics with a pseudo-rate constant which decreases as the initial pressure of nitrous oxide is increased. Gases initially added with the nitrous oxide decrease the pseudo-rate constant, whereas, oxygen pretreatment increases the pseudo-rate constant. The results are explained assuming Langmuir–Hinshelwood kinetics. Part of the surface is readily deactivated by oxide ions from nitrous oxide and oxygen, but additional active sites are created upon evacuation after exposure to oxygen.

There is no obvious trend in reactivity over the three oxides but there is a trend towards lower activity as the pressure is increased.

ACKNOWLEDGMENTS

Appreciation is expressed for the considerable help given by Dr. R. Rudham, Chemistry Department, Nottingham University, England. This work was partially financed by a grant from the National Research Council (Canada).

REFERENCES

1. Keenan, A. G., and Iyengar, R. D., *J. Catal.* **5**, 301 (1966).
2. Volpe, M. L., and Reddy, J. F., *J. Catal.* **7**, 76 (1967).
3. Amphlett, C. B., *Trans. Faraday Soc.* **50**, 273 (1954).
4. Dewing, J., and Cvetanović, R. J., *Can. J. Chem.* **36**, 678 (1958).
5. Cormack, D., Bowser, R. J., Gardner, R. F. G., and Moss, R. L., *J. Catal.* **17**, 230 (1970).
6. Roussel, Ph., and Teichner, S. J., *Catal. Rev.* **6**, 133 (1972).
7. Winter, E. R. S., *J. Catal.* **19**, 32 (1970).
8. Tanaka, K., and Ozaki, A., *J. Catal.* **8**, 307 (1967).
9. Cremer, E., and Marschall, E., *Monatsh. Chem.* **82**, 840 (1951).
10. Saito, Y., Yoneda, Y., and Makishima, S., *Actes Congr. Int. Catal., 2nd, 1960* 1937 (1961).
11. Winter, E. R. S., *J. Catal.* **15**, 144 (1969).
12. Watson, J. S., *Can. J. Technol.* **34**, 373 (1956).
13. Hoekstra, H. R., *Inorg. Chem.* **5**, 754 (1966).
14. Read, J. F., *Can. J. Chem.* **50**, 490 (1972).
15. Dunfield, L. G., and Read, J. F., *J. Chem. Phys.* **57**, 2178 (1972).
16. Linde, V. R., Margolis, L. Y., and Roginskii, S. Z., *Bull. Acad. Sci. USSR* **1**, 21 (1963).
17. Gay, I. D., and Tompkins, F. C., *Proc. Roy. Soc. Ser. A* **293**, 19 (1966).
18. Samaane, M., and Teichner, S. J., *Bull. Soc. Chim. Fr.* 1934 (1968).
19. Eley, D. D., *Nature (London)* **194**, 1076 (1962).
20. Balandin, A. A., and Tolstopiatova, A. A., *Int. Congr. Catal. 3rd*, **1**, 533 (1965).
21. Bakumenko, T. T., and Chashechnikova, I. T., *Kinet. Katal.* **10**, 796 (1969).
22. Sokolovskii, V. D., Mitrofanova, G. N., and Sazonov, L. A., *Kinet. Katal.* **11**, 804 (1970).
23. Winter, E. R. S., *J. Catal.* **22**, 158 (1971).
24. Gay, I. D., *J. Catal.* **17**, 245 (1970).